Oriented Crystallization in Fiber Formation: Inferences from the Structure and Properties of Melt Spun Syndiotactic Polypropylene Filaments

RAVI K. SURA, PRASHANT DESAI,* A. S. ABHIRAMAN

Schools of Textile & Fiber Engineering & Chemical Engineering, Polymer Education & Research Center, Georgia Institute of Technology, Atlanta, Georgia 30332

Received 28 February 2000; accepted 1 May 2000

ABSTRACT: In processes, such as melt spinning, the crystallization behavior of syndiotactic polypropylene (sPP) is found to be substantially different from that of most other linear polymers. The anisotropic stress field in such processes leads invariably to extension as well as alignment (orientation) of the chains in the melt, both of which contribute usually to dramatic enhancement in the rate of crystallization. However, since the primary structure of the sPP chain in its most preferred crystal form is comprised of a "coiled helical," —$(T_2G_2)_2$—, sequence, stress-induced chain extension can lead to conformational sequences that are not favorable for crystallization in this form. As a consequence, process conditions that generate higher stress levels can cause a diminution in the rate of crystallization of this polymer. Such conformation-related aspects of oriented crystallization of sPP have been addressed through an analysis of the structure and properties of melt-spun fibers, produced over a range of spinning speeds. The results serve to identify a refinement that is needed in current models of oriented crystallization and also a mechanism to promote the nucleation of crystallization of sPP. © 2001 John Wiley & Sons, Inc. J Appl Polym Sci 81: 2305–2317, 2001

Key words: oriented crystallization; syndiotactic polypropylene; melt spinning

INTRODUCTION AND LITERATURE

The highly regular primary structures of polymers that can be produced with relative ease using metallocene-based catalysts has led to renewed interest in the morphology and properties of such polymers. For example, although syndiotactic polypropylene (sPP) was first synthesized in 1960s by Natta et al.,[1] significant interest in the polymer did not result until the work of Ewen et al. in 1988,[2] which facilitated the production of highly syndiospecific polypropylene. Renewed research interest in sPP has produced several reports[3–23] on processing, structure, and properties of this polymer, and also on comparisons with its isotactic analog (iPP), a polymer that has been in large-scale production for approximately four decades. Among the various aspects of sPP, the most significant with regard to its applications pertains to its crystallization characteristics.

Crystalline Syndiotactic Polypropylene: Polymorphism and Chain Conformation

It is well known that sPP can exhibit polymorphism in its crystal structure. An important aspect in this regard is the set of three distinctly different chain conformations in these structures (Fig. 1), namely

Correspondence to: A. S. Abhiraman.
* *Present address:* FiberVisions, Inc., Covington, GA 30014.

Journal of Applied Polymer Science, Vol. 81, 2305–2317 (2001)

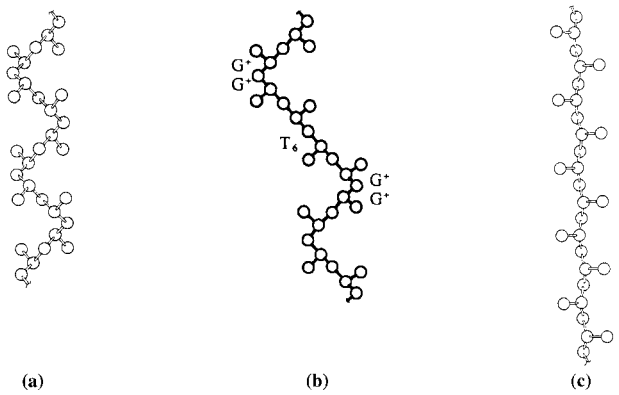

Figure 1 Chain conformational sequences in syndiotactic polypropylene crystals: (a) —$(T_2G_2)_2$—, (b) —$(T_6G_2T_2G_2)$—, and (c) all-*trans* —$(TTTT)_2$—.

(1) a highly coiled —$(T_2G_2)_2$— conformational sequence,[3–5,11–13,20,24] (2) a $(T_6G_2T_2G_2)$ conformational sequence,[8,18,19,21,22]and (3) an all-*trans* fully extended structure.[6,9,18,25,26] The various crystal forms of sPP, along with the corresponding conformational sequences, are summarized in Table I. It should also be noted here that the crystal densities increase with the more extended chain conformations. The crystal structure with all-*trans* chains, Form III in Table I, is reported to be obtained only upon cold-drawing,[6,9] a process that produces the highest level of chain extension and orientation. The extended structure, however, has been reported to be unstable; for example, it has been claimed to transform to a more stable structure, with —$(T_2G_2)_2$— repeat sequences, if heated to ~100°C or higher.[6,12,26]

Oriented Crystallization (in Fiber Formation)

The different extents of coiling of the chains in the various crystal structures of sPP, and the fact that a structure with one of the more coiled conformational sequences is more stable than those with fully extended chains, bring about an interesting aspect with regard to the role of stress-induced anisotropy in kinetics of crystallization of such polymers. Theories of oriented crystallization have almost invariably ignored such conformation-related effects, predicting only an increase— *often by several orders of mognitude*—in the rate of crystallization with increase in the strength of anisotropic stress field.[27–32] Such a prediction results from modeling the polymer chains as a sequence of freely orienting rod-like segments. In most linear polymers, with extended chains being the favored sequence for their incorporation into a crystal, a large increase in the rate of crystallization is indeed observed as a conse-

Table I Characteristics Parameters for Various Crystal Forms of sPP[a]

	Form I (Cell III)	Form I (Cell II)	Form II (Cell I)	Form III	Form IV
Chain conformation	s(2/1)2 helical —$(T_2G_2)_2$—	s(2/1)2 helical —$(T_2G_2)_2$—	s(2/1)2 helical —$(T_2G_2)_2$—	All-*trans* planar —(TTTT)—	—$(T_6G_2T_2G_2)$—
Unit cell	Orthorhombic	Orthorhombic	Orthorhombic	Orthorhombic	Triclinic
Cell dimensions	a = 14.5 Å b = 11.2 Å c = 7.4 Å	a = 14.5 Å b = 5.60 Å c = 7.4 Å	a = 14.5 Å b = 5.60 Å c = 7.4 Å	a = 5.22 Å b = 11.17 Å c = 5.06 Å	a = 5.72 Å b = 7.64 Å c = 11.6 Å α = 73.1° β = 88.8° γ = 112.0°
Space group	*Ibca*	*Pcaa*	$C222_1$	$P2_1cn$	$P1$ (or) $C2$
Crystal density	0.93 g/cm^3	0.93 g/cm^3	0.90 g/cm^3	0.945 g/cm^3	0.939 g/cm^3
X-ray peaks (CuKα)	12.2°, 15.8°, 18.8°, 20.6°	12.2°, 15.8°, 20.6°	12.2°, 16.6°, 20.6°	15.9°, 18.8°, 23.7°	12.9°, 16.8°, 19.9°
Solid state ^{13}C NMR peaks	21.0, 26.8, 39.6, and 48.3 ppm		18.9, 21.0, 22.4, 26.8, 39.6, 44.9, and 48.3 ppm	21.0, 28.9, and 50.2 ppm	19.8, 23.2, 40.2, 44.6, 49.0, and 50.2 ppm

[a] The nomenclature used here follows Rosa et al.[20]

quence of stress-induced orientational anisotropy. However, with polymers in which the preferred crystal structures are not composed of fully extended chains, higher intensity of anisotropic stress field can produce a predominance of conformational sequences that could be unfavorable for crystallization. If such a condition should exist, its manifestation would be seen clearly in processes, such as melt spinning, in which the polymer is oriented in an anisotropic stress field prior to its crystallization. Preliminary experiments in this regard showed that it was indeed likely to be the case with sPP.[33] Its manifestation was seen during the melt spinning process itself, with increased propensity for interfilament fusion at higher spinning speeds. Also, calorimetric and X-ray scattering analysis of as-spun fibers revealed reduced extents of crystallization at higher spinning speeds. A parallel, but independent, study by Gownder[34] regarding melt spun sPP fibers had reported that the fibers from melt spinning were sticky due to the slow rate of solidification, irrespective of quench conditions. In addition, the author had observed broad peaks in the wide angle X-ray diffraction (WAXD) spectra indicating low extent of crystallization and increasing packing disorder with spinning speed. These were in contrast to iPP, in which the crystallinity was seen to increase with spinning speed. These observations point clearly to the need for exploring the conformational structure of the sPP chains obtained in melt spinning and its effect on crystallization.

The primary goal of the present study is on enumerating the fundamental aspects of oriented crystallization of sPP. Inferences regarding possibly contrary influences of stress-induced extension and alignment of chains on crystallization, and on the consequent morphology and properties, have been obtained from a comprehensive analysis of the structure and thermorheological characteristics of sPP fibers, obtained by melt spinning at different speeds.

EXPERIMENTAL

Syndiotactic polypropylene (melt flow rate = 8 g/10 min at 230°C) was melt spun at 285°C on a research melt spinning line at a commercial research laboratory. The experimental setup consisted of a twin-screw extruder and a metering pump feeding a 7-hole spinneret. Take-up speed ranged from 200 to 2000 m/min, with the throughput adjusted to give a linear density of ~2.2 g/10,000 m (dtex) per filament.

Characterization Techniques

Helium pycnometry, WAXD, NMR, thermal analysis (DSC), mechanical testing, sonic pulse propagation, and thermorheological analyses (dynamic mechanical; thermal deformation/stress) were used to characterize the structure and properties of the melt spun fibers. A brief description of these techniques, including the conditions used, is given below.

Helium Pycnometry

A Quantachrome Helium Pycnometer (model MS-16) was used to measure the volume of a known mass of sPP fibers. Approximately 1–2 g (accurately weighed) of a sPP sample was packed in the sample sleeve of the helium pycnometer and enclosed in the sample cell. It was purged for 15–20 min to remove air and moisture before the measurement was made. After the sample cell was purged, the reference cell (fixed and known volume) was pressurized with helium to about 17 psi. Then, the gas was allowed to occupy both the reference and the sample cells and the final pressure reading was noted. The pressure difference between the final and initial states is used to calculate the volume of the sample (V_P), assuming that helium behaves like an ideal gas, as

$$V_P = V_C - V_R\left[\frac{P_1}{P_2} - 1\right]$$

where V_C is the cell volume, V_R is the reference volume, and P_1 and P_2 are the pressure above the ambient in the reference cell and the final lower pressure in the sample cell, respectively.

Wide-Angle X-Ray Diffraction

Flat plate WAXD photographs were obtained using a Rigaku-Geigerflex sealed tube X-ray generator. The radiation used was Ni-filtered Cu Kα and the system was operated at 45 kV and 25 mA, with a sample to film distance of 5 cm and exposure times of 1–3 h. The images were collected on an imaging plate phosphor screen from Molecular Dynamics.

A Rigaku-Rotaflex RU200 diffractometer with a rotating anode was used to obtain radial, equatorial, and azimuthal scans in the transmission

mode. The radial scans were obtained with the sample spinning around the beam axis to average orientational effects. The fibers were wound as a parallel array on a custom sample holder. The nominal wavelength of the Kα radiation used was 0.154 nm and a standard nickel filter attenuated the Kα component in the incident beam. The diffraction patterns were collected at 45 kV and 100 mA.

Nuclear Magnetic Resonance

All the NMR measurements were conducted on a Bruker DSX-300 spectrometer equipped with a double resonance magic angle spinning (MAS) probe head. Standard cross-polarization sequences were employed with a ^{1}H 90° pulse of 4 μs, contact time of 1 ms and a recycle delay of 3 s. One thousand twenty-four scans were accumulated to achieve good signal-to-noise averaging. A spinning speed of 5 kHz was employed for the sPP samples.

Calorimetry

DSC measurements were performed using a Seiko DSC Model 220C in nitrogen atmosphere. The samples consisted of approximately 10 mg of finely chopped fibers in aluminum pans. Unless otherwise specified, the scanning rate used was 5°C/min in both heating and cooling runs. Calibration was performed using an indium standard.

Mechanical Testing

Stress–strain curves were obtained using an Instron tensile tester model 1125. A gauge length of 11.4 cm and an elongation rate of 100% min^{-1} were employed.

Sonic modulus was computed from the sonic velocity through the yarns, obtained with the dynamic modulus tester PPM-5R from H. M. Morgan Company. An average of 5 readings was used to calculate the sonic modulus. The sonic modulus, E (in cN/dTex), is related to the sonic velocity, c (in km/s) by

$$E = 10 \times c^2$$

Dynamic Thermomechanical Analysis

Dynamic mechanical properties (storage and loss moduli; loss tangent) of the fibers were measured in tension, as a function of temperature, using a Seiko 210 Dynamic Mechanical Spectrometer. The conditions used were heating rate = 1°C/min; frequency = 3 Hz; sample length = 8 mm; strain amplitude = 20 μm. A constant base force was initially applied to the sample. It was adjusted during the test to compensate for the decrease in modulus with increasing temperature. The total force applied to the sample is given by

$$F_T = F + F_{\mathrm{GAIN}} \times F_{\mathrm{AMP}}$$

The base force was 150 g and F_{GAIN} and F_{AMP} were 1.5 and 30 g, respectively.

Thermal Deformation/Stress Analyses

Inferences regarding motions of chains in the intercrystalline amorphous regions can be obtained through the combination of thermal stress analysis (TSA) and thermal deformation analysis (TDA). In the case of fibers, these measurements consist of monitoring the temperature-induced changes in force at constant length (TSA), or in length at a constant force (TDA). The experimental apparatus consists of a temperature-controlled tubular heater, mounted on a mobile platform on wheels that can be moved rapidly over rails to enclose the loop of filaments being tested (Fig. 2). The fiber loop is connected at each end to Kevlar yarns, one of which is connected to a fixed support. In TSA, the other yarn is attached to a load cell for measuring the stress growth and/or relaxation. The test fiber, constrained to be at constant length, is enclosed by the heater that is initially at room temperature. The temperature is then increased at a constant rate (10°C/min in this study) and the consequent evolution of stress in the fiber is recorded as a function of temperature. The same procedure is used in nonisothermal deformation analysis, except that the other Kevlar yarn is passed over a smooth pulley and attached to a weight. A pointer is attached to the moving end so that the deformation in the test fiber as a function of temperature can be read against a scale. The corrections due to any changes in the Kevlar yarns are negligible in these experiments.

Shrinkage

The fibers were freely suspended in an air-circulated oven at 100°C for a specified time. The initial and final lengths were measured at room temperature, with the shrinkage calculated as

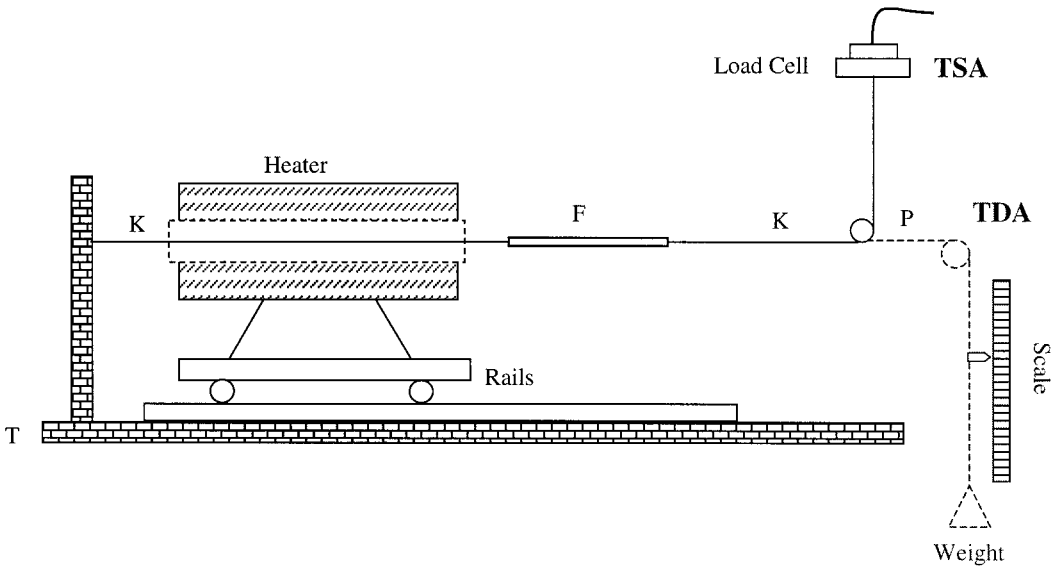

Figure 2 Schematic of apparatus for TSA and TDA: K, Kevlar ends; P, smooth pulley; T, table; and F, test filament loop. Heater can be moved on the rails to quickly enclose the fiber loop.

the percent change in length relative to the initial length.

RESULTS AND DISCUSSION

Preliminary Observations

The following set of initial observations are pertinent with regard to the structure and properties of the as-spun sPP fibers produced by melt spinning, spun at wind-up speeds ranging from 200 to 2000 m/min:

- The fibers tended to be fused to each other, especially at higher spinning speeds. This suggests that these fibers had not crystallized sufficiently to transform the polymer from a fluid-like to a solid-like state in the thread line.
- The density of as-spun fibers, measured through helium pycnometry, decreases with spinning speed (Fig. 3), showing clearly that the crystallinity decreases progressively when the spinning speed is increased from 200 to 2000 m/min.
- The flat plate WAXD photographs from all the fibers (Fig. 4) exhibit only diffuse reflections. Also, the peaks in the equatorial scans (Fig. 5) are broad, with only poorly resolved diffraction peaks. The differences, if any, point to slightly improved resolution of the diffraction peaks in the fibers formed at lower speeds. The [100] reflection (2θ = 12°) decreases in intensity and sharpness with increasing spinning speed. With respect to the crystal structure, the [010] reflection (2θ = 16.6°), albeit broad, reveals the packing mode of form II, which occurs in oriented systems.[18,19,24,34]
- The DSC scans of all the fibers exhibit distinct cold crystallization exotherms, beginning around 75°C (Fig. 6). In addition, an endothermic peak is observed around 45°C.

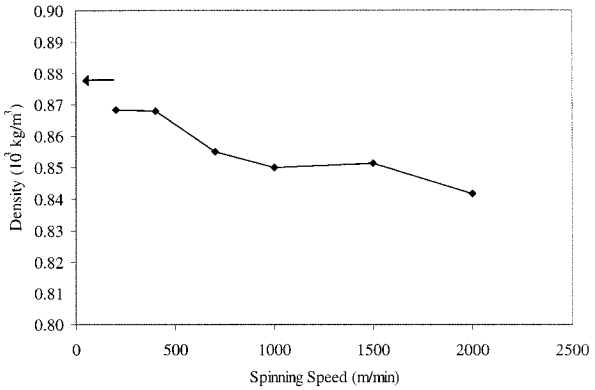

Figure 3 Bulk density of syndiotactic polypropylene melt-spun fibers. Density of sPP pellets is marked by an arrow on the *y* axis.

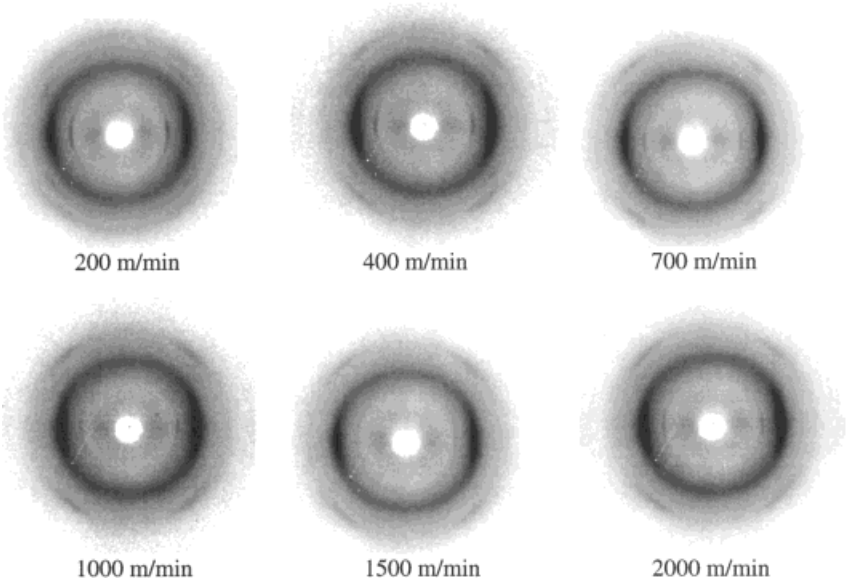

Figure 4 Flat plate X-ray photographs of sPP fibers melt spun at different speeds. The fiber axis is vertical in all cases. Ni-filtered CuKα radiation was used with a sample to film a distance of 5 cm and exposure time of l h.

Nakaoki et al.[35] have attributed this peak to the transformation of *trans* to coiled helical conformational sequences.

The above set of observations confirm the fact that the as-spun sPP fibers have only a low extent of crystallization and crystal orientation, with a significant potential for additional crystallization above what appears to be a conformation-related enthalpic change that occurs around 45°C.

Structure of As-Spun Fibers

In order to examine the conformational sequences developed in melt spinning of sPP, solid-state cross-polarization/MAS (CP/MAS) ^{13}C NMR spectra of the as-spun fibers were compared with those from melt- and solution-cast samples (Fig. 7). The coiled —$(T_2G_2)_2$— conformational sequence in sPP would result in two equally probable, distinct sites for the methylene group, with a large difference of the chemical shifts of the two arising mainly due to the dissimilar three-bond interactions on each type of methylene carbon.[36] The NMR spectra of melt-cast and solution-cast sPP indeed show the splitting of the methylene peaks (39.3 and 48.1 ppm), characteristic of the —$(T_2G_2)_2$— conformational sequence,[36,37] along with peaks at 21.1 ppm (methyl carbon) and at

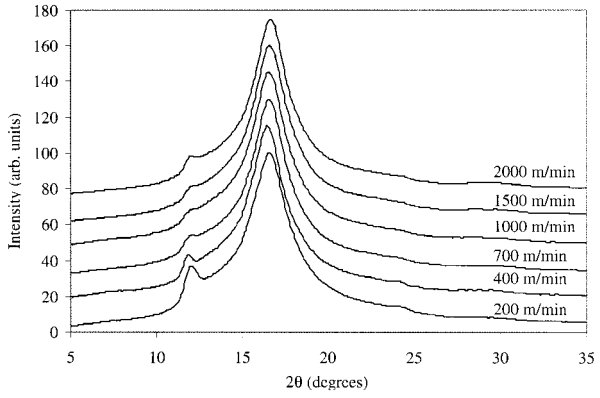

Figure 5 Equatorial WAXD diffractograms of sPP fibers melt spun at different temperatures.

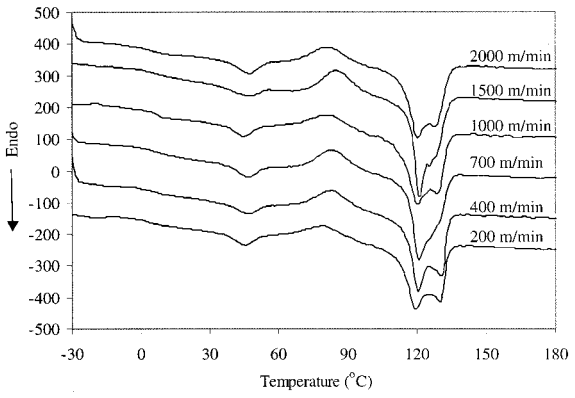

Figure 6 DSC (first heating) scans of sPP melt-spun fibers; heating rate = 5°C/min.

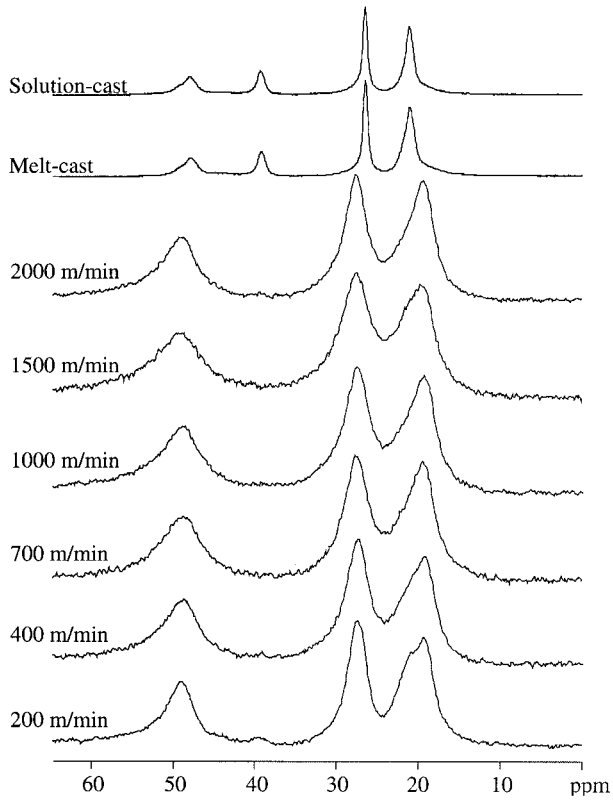

Figure 7 CP/MAS ^{13}C NMR spectra of sPP fibers melt spun at different spinning speeds as well as solution-cast and melt-cast samples. ^{1}H 90° pulse = 4μs; contact time = 1 ms; recycle delay = 3 s; spinning speed = 5 kHz.

26.5 ppm (methine carbon). However, the —$(T_2G_2)_2$— induced splitting is essentially absent in the spectra of all but one of the fibers. The NMR spectrum of the fibers melt-spun at the lowest speed, 200 m/min, exhibits a small peak around 39 ppm, indicating the presence of some helical conformational sequences. The spectra of all the sPP fibers show peaks at 19, 27, and 48 ppm, along with a shoulder at 21 ppm on the methyl peak. Such a spectrum with a single distinct methylene peak (48 ppm) arises from a mostly —(TTTT)— conformation.[18,19,21,22,37] The methylene carbons do not receive any *γ-gauche* effect in the *trans* planar conformation and exhibit only a single peak. These data point to the fact that the tensile stress in melt spinning causes the chains to be extended into predominantly *trans* conformations, especially at higher speeds. While this aspect is similar to other polymers, its effect on crystallization of sPP in the melt-spinning threadline is different from that of most polymers.

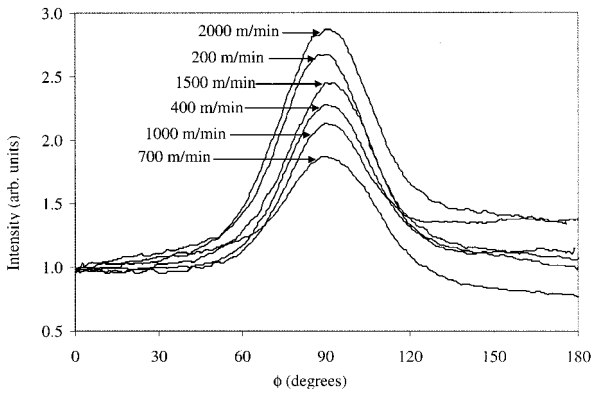

Figure 8 Azimuthal scans at 2θ = 16.6° for sPP fibers melt spun at different speeds.

Stress-induced uniaxial anisotropy in most linear polymers causes a dramatic increase in the rate of crystallization and leads to a high crystal orientation along the preferred direction.[28,29,38,39] However, if sPP should have a strong preference to crystallize in a form with its chains in a coiled helical sequence, any favorable effect on crystallization from increased interchain alignment could be negated by the unfavorable conformational sequences introduced by the stress in a melt spinning thread line. In addition to the X-ray flat plate photographs and the scattering intensity profiles (Figs. 4 and 5) described earlier, which reveal only a low extent of crystallization in the as-spun fibers, the unusual aspect of sPP crystallization in this regard is further exemplified by the azimuthal scans of the [100] reflection, shown in Fig. 8. The crystal orientation of all the as-spun sPP fibers is low, with the full width at half the maximum intensity (FWHM) of all the azimuthal scattering intensity profiles around 30°–40° (Ta-

Table II FWHM (in Degrees) of Azimuthal X-Ray Scattering Intensity Scans at 2θ = 12° ([100] Reflection) for As-Spun, Constant Length Annealed (CLA), and Free Length Annealed (FLA) sPP Fibers

Spinning Speed (m/min)	As-Spun Fibers	CLA Fibers	FLA Fibers
200	34	22	26
400	33	23	28
700	41	18	21
1000	44	22	24
1500	37	16	25
2000	39	18	29

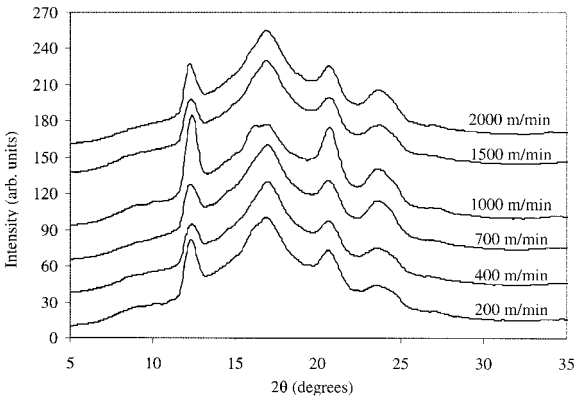

Figure 9 Radial WAXD diffractograms for constant length annealed (CLA)—at 100°C—sPP melt-spun fibers.

ble II). Such a low orientation of the crystals formed from oriented precursor fibers, and its relative insensitivity to the spinning speed, clearly implies that their formation is not dictated by the most-oriented segments that are also likely to be the most extended.

That crystallization of sPP in its preferred form is not facilitated in the usual manner by chain orientation/extension is seen further in the structure of the fibers that result from inducing crystallization by constant-length annealing at 100°C. Annealing at this temperature produces well-crystallized fibers in all cases, as revealed by the distinct diffraction peaks in the radial x-ray scattering intensity profiles (Fig. 9), and the absence of cold-crystallization exotherm in the DSC scans (Fig. 10). However, the following should be noted regarding the morphology and the crystal structures produced. Their NMR spectra (Fig. 11) show the splitting of the methylene peaks, indicating that crystallization has occurred with conversion of the predominantly all-*trans* conformational sequences of the as-spun fibers to coiled —$(T_2G_2)_2$— sequences on annealing. The overall orientation and chain extension introduced during melt spinning of these fibers is apparently insufficient to induce them to crystallize in the otherwise less preferred Form III (Table I), with its extended chain structure. However, it should be noted here that the postspinning crystallization of these fibers has been carried out at 100°C, a temperature around which even already formed Form III crystals, with their all-*trans* conformations, have been reported to transform to one with coiled —$(T_2G_2)_2$— sequences.[19] The increased crystallinity results in an increase in the crystal orientation, as seen by the decreased FWHM values of the azimuthal scans ($2\theta = 12°$) of the constant length annealed samples (Table II), when compared to the as-spun samples, namely, 30°–40° and ~20°, respectively.

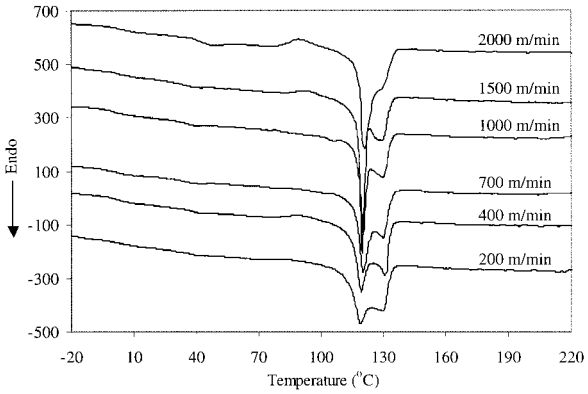

Figure 10 DSC (first heating) scans of CLA—at 100°C—sPP melt-spun fibers. Heating rate = 5°C/min.

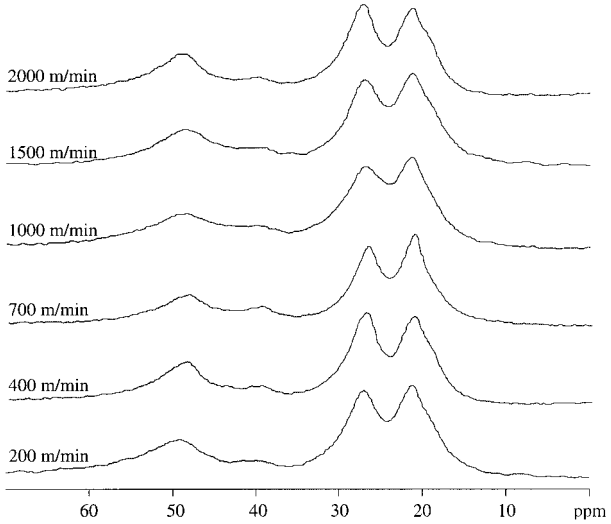

Figure 11 CP/MAS ^{13}C NMR spectra of CLA—at 100°C—sPP fibers melt spun at different speeds. NMR run under same conditions as specified in Figure 7.

The essential inferences from the above-discussed experimental results can be summarized as follows:

1. The stress field prior to crystallization in fiber formation causes the sPP chains to assume extended conformational sequences that are unfavorable for crystallization in its naturally preferred form.
2. The chain extension in melt spinning is, however, not sufficient to induce it to crys-

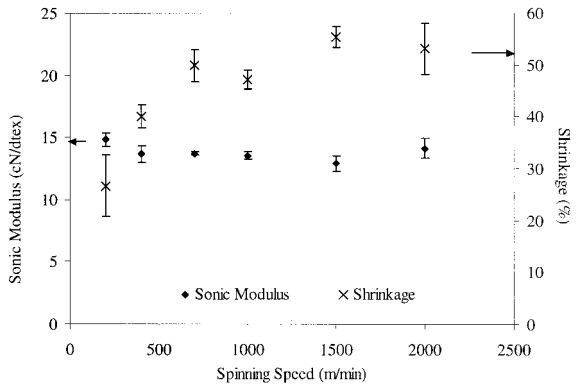

Figure 12 Sonic modulus and shrinkage (in air at 100°C) of melt-spun sPP fibers as a function of spinning speed.

tallize to a significant extent in its less preferred form that is made up of all-*trans* conformational sequences.

3. Unlike the case with most linear polymers, the stress-induced orientation in the melt zone does not produce high crystal orientation in sPP, most likely due to the fact that formation of the preferred crystal structure is not dictated or facilitated by the most oriented or most extended segments.
4. Annealing (at 100°C) produces a solid-state structure of sPP that is well crystallized in its preferred form, with coiled —$(T_2G_2)_2$— conformational sequences.

Structure and Thermorheological Responses

The structural inferences regarding as-spun sPP fibers have been verified against the thermorheological responses and mechanical properties of the as-spun and annealed fibers. The following are significant in this regard:

- The free shrinkage at 100°C is high for all the fibers, increasing from 25 to 55% as the spinning speed is increased from 200 to 2000 m/min (Fig. 12). This is consistent with the combination of the stress-induced orientation in the melt zone of the thread line, expected in all polymers, which should increase with spinning speed, and the fact that the as-spun fibers are all of low crystallinity. However, the following important fundamental difference between typical polymers and sPP should be noted. While the tendency to shrink at temperatures well above T_g is a natural consequence of oriented noncrystalline segments in all polymers, the magnitude of actual shrinkage that results from it would depend on the degree to which the oriented segments can coil in the process. Since, in most polymers, high orientation also results in high rate of crystallization, the shrinkage is often limited by crystallization, with preferential transformation of the more oriented noncrystalline segments. For example, melt-spun polyethylene terephthalate exhibits a pronounced maximum in shrinkage as a function of spinning speed, with a dramatic reduction in shrinkage caused by even a low extent of crystallization that occurs at high spinning speeds.[40–42] Also, the free shrinkage of polymers, such as nylon 66, polyethylene, and isotactic polypropylene, which invariably crystallize in a melt-spinning thread line, is low at all spinning speeds. However, in the case of sPP, with the coiled helix in its preferred crystal structure, a significant shrinkage would result, irrespective of any crystallization *during* the annealing process. The formation of coiled helical conformational sequences and the increased crystallinity can be clearly observed, respectively, in the NMR spectra (Fig. 13) and the radial X-ray scattering intensity profiles (Fig. 14) of the free length annealed samples.
- The low extent of crystallization in the as-spun fibers, the apparent enthalpic relaxation observed around 45°C and the motions that facilitate the onset of significant crystal-

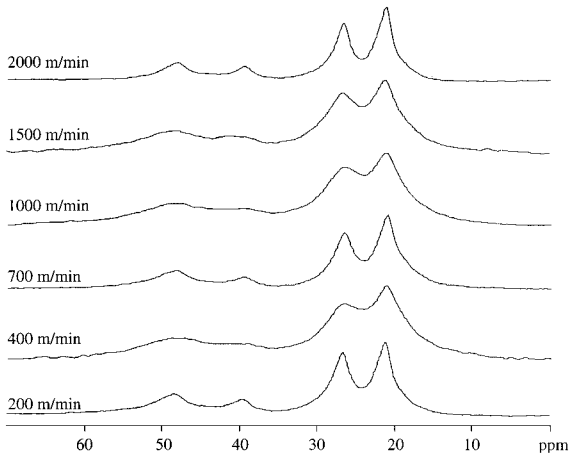

Figure 13 CP/MAS ^{13}C NMR spectra of free length annealed (FLA)—at 100°C—sPP fibers melt spun at different speeds. NMR run under same conditions as specified in Figure 7.

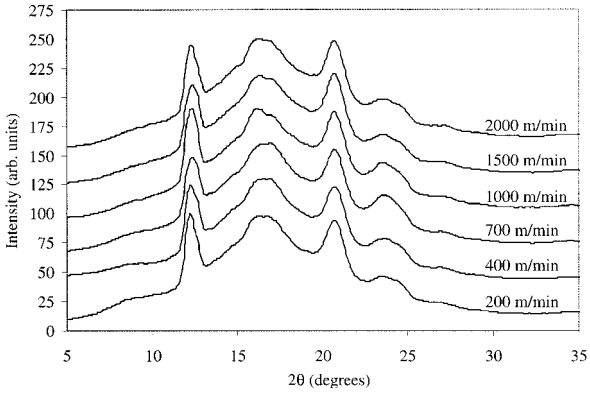

Figure 14 Radial WAXD diffractograms for FLA—at 100°C—sPP fibers melt spun at different speeds.

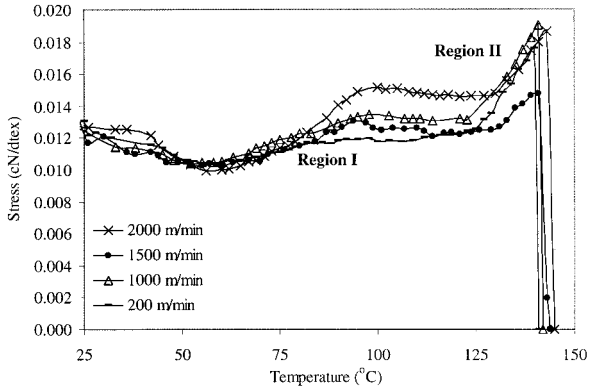

Figure 16 Nonisothermal stress analysis of sPP fibers melt spun at different speeds; heating rate = 10°C/min. The different regions are explained in the text.

lization around 75°C are reflected, together, in the dynamic mechanical spectra (Fig. 15). The loss (tanδ) process in these spectra, from ~−10 to ~70°C, is unusually broad, yet intense, for a homopolymer. It should also be noted that the spectra for the fibers melt-spun at higher speeds had to be limited to temperatures below ~90°C due to failure of the samples, indicating again the low extent of crystallization in the fibers melt-spun at the higher spinning speeds. The spectra for the annealed fibers are, as expected from their crystallized structure, of substantially reduced intensity (Fig. 15).

- A clear manifestation of the extended "all-*trans* → coiled helix" transformation due to crystallization of these melt-spun sPP fibers is seen in the two thermorheological measurements, TSA and TDA. The nonisothermal stress spectrum (Fig. 16) shows an initial decrease from the applied pretension, due to the combination of thermal expansion and, possibly, relaxation of some unconstrained segments. There is a distinct increase (Region I; Fig. 16) in the shrinkage force, beginning around 65°C, which coincides with the onset of cold crystallization (Fig. 6—DSC). The fact that, after the completion of cold crystallization, this force remains essentially constant until the onset of melting suggests that it is primarily a manifestation of the coiling required for crystallization. As expected, there is a further increase in the thermal stress (Region II; Fig. 16) with the progression of melting of the oriented crystals, due to the fact that there is an additional coiling potential of the noncrystalline segments that are generated from melting of the crystals. Above ~140°C, the shrinkage force drops precipitously due to the loss of structural integrity from large-scale melting of the fiber.

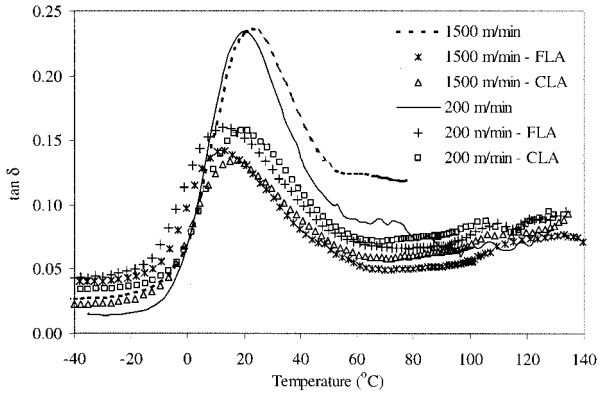

Figure 15 Representative DMA (loss tangent) scans of as-spun and annealed (at 100°C) sPP fibers.

There are at least two fundamental phenomena that influence the evolution of shrinkage force when the as-spun fibers are heated (Region I) to temperatures above glass transition[30,31]:

1. The well-known tendency of oriented noncrystalline segments to coil, which produces a shrinkage force. Its evolution, and possibly simultaneous or subsequent devolution, would be governed by the orientation, temperature, and the extent to which constraints from crystals can inhibit relaxation of orientation.

2. Additional crystallization that can occur if the precursor fiber is incompletely crystallized.

- While the effect of the first phenomenon is the same in all polymers, the consequences of crystallization would depend on the conformations of chains in the crystal structures vis-à-vis those of the precursor chains. If the chain in the crystal should exist in its most extended conformational sequence, as is the case with most linear polymers, the effect of onset of crystallization would be to diminish the shrinkage force. On the other hand, if the chain conformation in the crystal structure is a coiled helix, such as the case in preferred sPP structures, the consequence of crystallization from an oriented precursor would be to increase the shrinkage force. This is due to the "extended chain → coiled helix" conformational transformation required for their crystallization. However, in all cases, the constraints from the crystals produced and their melting near T_m can lead to the evolution of a higher shrinkage force (Region II; Fig. 16) as the temperature is increased toward melting.
- The response in nonisothermal deformation analysis (Fig. 17) is also entirely consistent with the inferences drawn from morphological observations. The TDA profile exhibits a significant shrinkage in the length of the fibers, beginning around 65°C, which coincides with the observed onset of crystallization (Fig. 6). It corresponds to the increase in the shrinkage force in TSA (Region I; Fig. 16). The higher extent of chain extension obtained at the higher spinning speeds is clearly reflected in the significantly higher shrinkage. Also, as expected, the onset of melting around 130°C produces substantial additional shrinkage in the fibers.
- The sonic modulus remains essentially constant with spinning speed (Fig. 12), again due to the combination of increasing noncrystalline orientation, but reduced extent of crystallization, obtained at increasing speeds. The relative insensitivity of both breaking elongation and strength to changes in spinning speed (Fig. 18) are also consistent with the inferences that have been made regarding the evolution of structure in melt spinning of sPP.

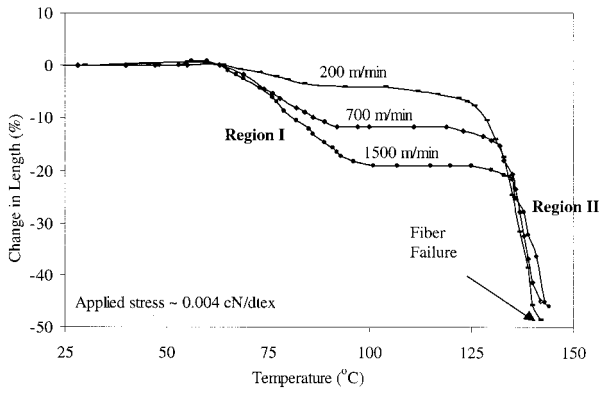

Figure 17 Nonisothermal deformation analysis of sPP fibers melt-spun at different speeds; heating rate = 10°C/min. The different regions are explained in the text.

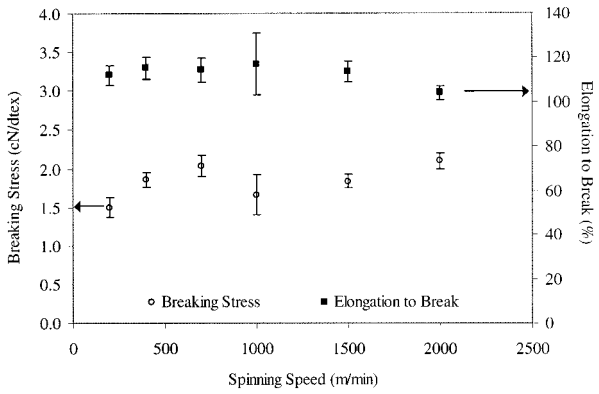

Figure 18 Tensile properties—breaking stress and elongation to break—of sPP melt-spun fibers. Rate of extension = 100% min^{-1}; gage length = 11.4 cm.

Thus, in the case of syndiotactic polypropylene, an increase in orientation does not *ipso facto* lead to an increase in its rate of crystallization. The stress-induced *reduction* in the concentration of coiled helical conformational sequences, which constitute the primary chain structure in sPP's preferred crystal structure, is likely to be the cause for the decrease, instead of an increase, in the rate of crystallization with spinning speed.

SUMMARY AND CONCLUSIONS

The current study of evolution of structure and properties in melt extrusion of syndiotactic polypropylene has provided the following set of observations and inferences of both fundamental and practical significance.

- Melt spun sPP fibers are poorly crystallized. An increase in the spinning speed results only in a reduction in the extent of oriented crystallization. Also, contrary to the nature of most linear polymers, the higher stresses at increasing spinning speed do not necessarily lead to a higher crystalline orientation. These are consistently reflected in measurements with helium pycnometry, wide-angle x-ray scattering, differential scanning calorimetry, and free shrinkage.
- Solid-state NMR measurements show that the structures produced in as-spun sPP fibers have predominantly extended conformational sequences, more so at higher spinning speeds. The combination of chain extension and orientational alignment of chains would lead to a dramatic increase in the rate of crystallization of most linear polymers. However, in the case of syndiotactic polypropylene, with its preference for crystallization in a structure that is comprised of coiled —$(T_2G_2)_2$— conformational sequences, chain extension could hinder such a transformation. The overall kinetic effect of anisotropic stress fields, such as that which exists in a melt spinning process, would be dictated by the relative effects of the rate-enhancing chain alignment *and*, possibly, rate-diminishing chain extension.
- If heated to temperatures much above room temperature, as-spun sPP fibers undergo a significant extent of crystallization, accompanied by extended α-helical conformational transformation and a substantial shrinkage in length. This shrinkage, which increases with spinning speed, is usually the manifestation of the natural tendency of all oriented flexible polymer molecules to coil. However, in the case of polymers like sPP, with their preference for crystallization in structures with coiled conformational sequences of the chains, shrinkage in the oriented precursor could also occur predominantly as a consequence of this phase transformation.
- The structure-related observations with sPP fibers show clearly a deficiency in current theories of stress-induced oriented crystallization in fiber formation, namely, the absence of consideration of the conformational sequences that are formed in the melt zone vis-à-vis the sequences that might be preferred for crystallization in the subsequent zone. Thus theories, such as those of Ziabicki et al.[28,29] and Abhiraman et al.,[38,39] have to be revised to incorporate this aspect, especially with regard to polymers that prefer to crystallize with coiled helical chains in them. Induced chain extension in such polymers can cause a reduction in the rate of crystallization, in spite of the higher degree of orientational alignment that might be achieved.

The above-mentioned observations and inferences are being utilized to reformulate theories of oriented crystallization and also to design appropriate processes to realize optimum properties in melt spun and/or drawn fibers of syndiotactic polypropylene. An interesting option with regard to the latter is nucleation that can be obtained in blends of sPP with polymers that crystallize at higher temperatures than sPP and also whose crystallization is *facilitated* by stress-induced orientation. Results from experiments on sPP that has been blended with low concentrations of iPP are presented in a companion report.[43]

REFERENCES

1. Natta, G.; Pasquon, I.; Zambelli, A. J Am Chem Soc 1962, 84, 1488.
2. Ewen, J.; Jones, R.; Razavi, A.; Ferrara, J. J Am Chem Soc 1988, 110, 6255.
3. Lotz, B.; Lovinger, A. J.; Cais, R. Macromolecules 1988, 21, 2375.
4. Lovinger, A. J.; Lotz, B.; Davis, D. Polym Prepr 1990, 33, 270.
5. Lovinger, A. J.; Lotz, B.; Davis, D. Polymer 1990, 31, 2253.
6. Chatani, Y.; Maruyama, M.; Noguchi, K.; Asanuma, T.; Shiomura, T. J Polym Sci Part C—Polym Lett 1990, 28, 393.
7. Haftka, S.; Konnecke, K. J. Macro Sci—Phys 1991, B30(4), 319.
8. Chatani, Y.; Maruyama, M.; Noguchi, K.; Asanuma, T.; Shiomura, T. J Polym Sci Part B—Polym Phys 1991, 29, 1649.
9. Sozzani, P.; Galimberti, M.; Balbontin, G. Makromol Chem Rapid Commun 1992, 13, 305.
10. Peacock, A. J. U.S. Patent 5,272,003, 1993.
11. Lovinger, A. J.; Lotz, B.; Davis, D.; Padden, F. J. Macromolecules 1993, 26, 3494.
12. De Rosa, C.; Corradini, P. Macromolecules 1993, 26, 5711.
13. Lovinger, A. J.; Lotz, B.; Davis, D.; Schumacher, M. Macromolecules 1994, 27, 6603.
14. Asanuma, T.; Shiomura, T.; Kimura, S.; Uchikawa, N.; Kawai, Y.; Suchiro, K.; Fukushima, S. U.S. Patent 5,474,646, 1995.

15. Asanuma, T.; Shiomura, T.; Kimura, S.; Uchikawa, N.; Kawai, Y.; Suchiro, K.; Fukushima, S. U.S. Patent 5,624,621, 1997.
16. Sakata, Y.; Unwin, A. P.; Ward, I. M. J Mat Sci 1995, 30, 5841.
17. Robriguez-Arnold, J.; Bu, Z.; Cheng, S. Z. D. J Macro Sci Rev Macro Chem Phys 1995, C35(1), 117.
18. Auriemma, F.; Lewis, R.; Spiess, H. W. Macromol Chem Phys 1995, 196, 4011.
19. Auriemma, F.; Born, R.; Spiess, H. W.; De Rosa, C.; Corradini, P. Macromolecules 1995, 28, 6902.
20. De Rosa, C.; Auriemma, F.; Corradini, P. Macromolecules 1996, 29, 7452.
21. Asakura, T.; Aoki, A.; Date, T.; Demura, M.; Asanuma, T. Polym J 1996, 28(1), 24.
22. Auriemma, F.; De Rosa, C.; Ballesteros, O. R.; Corradini, P. Macromolecules 1997, 30, 6586.
23. Asanuma, T.; Sasaki, T.; Ito, M.; Shiomura, T. U.S. Patent 5,759,469, 1998.
24. Corradini, P.; Natta, G.; Ganis, P.; Temmusi, P. A. J Poly Sci Part C 1967, 16, 2477.
25. Natta, G.; Corradini, P.; Ganis, P. Makromol Chem 1960, 39, 238.
26. Natta, G.; Peraldo, M.; Allegra, G. Makromol Chem 1964, 75, 215.
27. Krigbaum, W. R.; Roe, R. J. J Polym Sci Part A 1964, 2, 4391.
28. Ziabicki, A.; Jarecki, L. Colloid Polym Sci 1978, 256, 332.
29. Ziabicki, A.; Jarecki, L. In High Speed Fiber Spinning; Ziabicki, A., Jarecki, L., Eds.; John Wiley & Sons: New York, 1985.
30. Desai, P.; Abhiraman, A. S. J Polym Sci Part B Polym Phys Ed 1989, 27, 2469.
31. Agarwal, U. S.; Asher, P.; Carr, W. W.; Pinaud, F.; Desai, P.; Abhiraman, A. S. In Polymer and Fiber Science: Recent Advances; Fornes, R. E.; Gilbert, R. D., Eds.; VCH Publishers: New York, 1992; Chap 5.
32. Desai, P. Ph.D. thesis, Georgia Institute of Technology, 1988.
33. Sura, R. K.; Desai, P.; Abhiraman, A. S. ANTEC Conf Proc 1999, 1764.
34. Gownder, M. ANTEC Conf Proc 1998, 1511.
35. Naokaoki, T.; Ohira, Y.; Hayashi, H.; Fumitaka, H. Macromolecules 1998, 31, 2705.
36. Bunn, A.; Cudby, M.; Harris, R.; Packer, K.; Say, B. J Chem Soc, Chem Comm 1981, 15.
37. Sozzani, P.; Simonutti, R.; Galimberti, M. Macromolecules 1993, 26, 5782.
38. Abhiraman, A. S.; Hagler, G. E. J Appl Polym Sci 1987, 33, 809.
39. Abhiraman, A. S. J Polym Sci B Polym Phys 1983, 21, 583.
40. Hamidi, A.; Abhiraman, A. S. J Appl Polym Sci 1983, 28, 567.
41. Desai, P.; Abhiraman, A. S. J Polym Sci 1985, 23, 653.
42. Ziabicki, A.; Kawai, H., Eds. High Speed Fiber Spinning; John Wiley & Sons: New York, 1985; pp 95 and 429.
43. Sura, R. K.; Desai, P.; Abhiraman, A. S. Submitted.